J. Indian Chem. Soc.,
Vol. 93, February 2016, pp. 151-157

Examining the physical characteristics and preparation of nano-modified materials of kaolinite clay catalyst

Shu-Lung Kuo[a] and Edward Ming-Yang Wu*[b]

[a]Engineering Consultant, Kelee Environmental Consultant Corporation, 6F.-2, No. 288-8, Sinya Road, Kaohsiung City 806, Taiwan

E-mail : singsuey@ms28.hinet.net *Fax* : 886-7-8150816

[b]Department of Civil and Ecological Engineering, I-Shou University, No. 1, Sec. 1, Syecheng Rd., Daishu District, Kaohsiung City 840, Taiwan

E-mail : edmywu@isu.edu.tw

Manuscript received online 08 January 2015, revised 28 January 2015, accepted 11 May 2015

Abstract : Kaolinite clay was adopted as the research topic for this study, which is to examine the exchange of Ag^{+}, Zn^{2+} and Ti^{4+} to kaolinite through an ion exchange scheme so that it alters the quality of its surface and forms the nano-grade kaolinite clay catalyst, and also to investigate its physical characteristics through the X-ray diffraction analysis, transmission electron microscopy (TEM) and differential thermal scanning calorimeter, thermogravimetric analyzer (DSC-TGA).

All catalysts went through the calcination process and were observed by TEM, indicating that the sizes of the catalyst particles on the kaolinite clay carrier for all catalysts were between 20 to 100 nm, thus proving that these catalyst particles do exist in the kaolinite after ion exchange, as well as that they are unquestionably nano-grade.

The results revealed that the presence of a certain amount of metal species may offer a prospective "green chemistry" strategy in the traditional preparation processes.

Keywords : Kaolinite, kaolinite clay catalyst, X-ray, thermal analysis, TEM.

Introduction

A photocatalyst is a material capable of exercising the catalyst function by utilizing photo energy that activates chemical reactions in its surroundings. The photocatalyst reaction utilizes a semiconductor as a photocatalyst that follows the steps of converting photo energy into chemical energy. The semiconductor materials generally adopted as a photocatalyst include : TiO_2, ZnO, CdS, SnO_2, WO_3, etc. The optical properties of the semiconductors will be affected by various energy band structures. Generally speaking, semiconductors with a larger energy gap may have higher activity while also needing to consume more energy in order to be activated. If the energy gap is too small, then the activated electron-hole pairs can be re-joined, thus causing poor activity. Among these, TiO_2 has a high degree of stability. Its properties will not be easily changed in acidic or alkaline environments; thus, presenting beneficial characteristics : harmless, safe and an excellent energy gap[1]. Given its minor effect on human body and the natural environment, it has become a widely applied photocatalyst material.

Many researchers have been attempting to modify the catalyst surface to increase the efficiency of these processes. To increase the adsorption capacity of organic compounds, researchers have explored supporting ZnO, Ag_2O or TiO_2 on such porous materials as silicon dioxide (SiO_2)[2,3], zirconiumoxide (ZrO_2)[4,5], quartz[6], zeolites, activated carbon (AC)[7,8], and carbon nanotubes (CNTs)[9,10]. Among the methods of immobilization studied are chemical vapor deposition (CVD), impregnation, plasma coating, sol-gel, mechanical coating, microemulsion, and mixing nano-ZnO with AC at different proportions in an aqueous suspension[8,11,12]. ZnO-coated carbon nanotubes, using the filtered cathodic

vacuum arc technique, and the growth of ZnO nanowires on modified, well-aligned CNT arrays using a hydrothermal process have also been studied[13,14]. Spherical AC containing ZnO, prepared using both strong and weak acid ion-exchange resins as starting materials, has shown high humic acid removal efficiency[15]. Although AC is temperature sensitive and can be oxidized in the air at higher temperatures, when it is used as a photocatalyst support, heat-treatment is required.

The main focus of this study is on adopting kaolinite as a major catalyst carrier and exchanging Ag^{+}, Zn^{2+}, and Ti^{4+} for the catalyst carrier by an ion exchange process so that it forms the so-called clay photocatalyst, and also by adopting instruments like X-Ray diffraction analysis (XRD), transmission electron microscopy (TEM) and differential thermal scanning calorimeter thermogravimetric analyzer (DSC-TGA) to examine the classification and characteristics of various physical properties of the kaolinite catalyst.

Research method and preparation of materials :

The purification and preparation of sodium saturated kaolinite :

Measure 60 g of commercially available kaolinite to place into a two-liter size beaker; then add 1.8 L of de-ionized water to have it expand completely by first stirring before soaking it for several days. After it has expanded, take 250 mL of the kaolinite suspended solution from the beaker and filter sand particles using 300-mesh grade wet sieving so that the filtered solution is moved into a long sedimentation cylinder with a capacity of 1 L. Add de-ionized water to 1 L solution and vigorously stir with an agitating impeller before leaving to stand still for natural sedimentation. After eight hours, extract the top 10 centimeters of the suspended solution in the sedimentation cylinder by siphonage. Then the suspension solution is subsequently centrifuged in an 18000 rpm high-speed centrifuge.

After being centrifuged, the kaolinite will be furthered saturated with 1 *M* sodium chloride (NaCl), i.e. adding an appropriate amount of the sodium chloride solution and shaking continuously for eight hours, and washing with de-ionized water three times. After the processes noted above, it will be further washed with 95% ethanol to exclude excessive chloride ions in the clay. A process of rinsing with ethanol will be repeated as necessary until no chloride salt exists. The saturated kaolinite will be further frozen for dehydration and ground in an agate mortar into powder in order to produce saturated sodium clay.

Preparation of kaolinite-Ag and kaolinite-Zn :

First prepare solutions of $AgNO_3$ and $ZnCl_2$ with a density of 0.1 *N* and then add clay with a density of 2%, while using the water bath approach to maintain the temperature at 40 °C, stirring uniformly for 48 h. It will be stirred further at 80 °C for another 2 h. The upper part of the solution will be discarded after being left to stand still for a certain time. The kaolinite-Ag and kaolinite-Zn catalysts complete modification will be dehydrated using the frozen dehydration method. It will be ground before further sintering at 350 °C within a furnace for 2 h. It can be stored for later utilization after it has cooled down to normal room temperature.

Preparation of kaolinite-Ti :

Kaolinite-Ti is prepared first by taking 1.09 mL of $TiCl_4$ for dissolving into water to produce a solution of $TiCl_4$ with a density of 0.1 *N*. Subsequently, 2% of the clay is added into the solution and a water bath is used to maintain the temperature at 40 °C, and is uniformly stirred for 48 h. It is stirred at 80 °C for another 2 h. The upper part of solution will be discarded after standing for a certain time. It will also be washed with 95% ethanol to exclude excessive chloride ions in the clay. The final kaolinite-Ti catalyst modification is dehydration using the frozen dehydration method. It will be ground before further sintering in the 350 °C furnace for 2 h. It can be stored for later utilization after it has cooled down to normal room temperature.

X-Ray diffraction analysis :

The X-ray diffraction analysis utilizes the X-ray diffractometer coded with Rigaku RINT 2000 to conduct the analysis. The CuK_{α} is used as a photo source to separately analyze the crystalline forms of kaolinite clay and the other four clay catalysts after modifications in order to explore spacing of layers for these materials. The wavelength of the X-ray produced is 1.5418 Å and 10 mA for testing operational current, 20 kV fr voltage, 5 deg/min for a scanning rate with a scanning angle of $2\theta = 2\sim40°$.

Transmission electron microscope analysis (TEM analysis) :

The transmission electron microscope was utilized to

observe the particle diameters and distribution patterns of various clay catalysts for this study. The instrument is coded HR-TEM 2100. Steps for producing samples for testing : first a sample with a scale of around 0.1 g is put into a centrifuge tube and alcohol is added with a density of 50% for about 10 mL. The centrifuge tube is subsequently placed in a beaker with water and shaken in the supersonic vibrator for 30 min. The needed samples are collected from the suspension in the centrifuge tube with static dissipative tip pair clamping carbon-coated copper mesh; this is done twice and samples are left to stand still before further analysis.

Thermal analysis (TA) :

The differential scanning calorimeter thermogravimetric analyzer is utilized for this study to produce various heating rates for the thermal analysis of a range of clay catalysts. This instrument can test the performances of DSC or TGA at high temperatures for materials either in solid, powder, gel or liquid states. The analysis steps are listed as follows :

(1) Sample preparation : All catalyst samples for testing should be ground in an agate mortar before being fully dehydrated. Subsequently, 5 to 20 mg size samples are taken and filled into a platinum plate before testing.

(2) Analysis conditions : Adopting nitrogen as the purge gas with a heating rate of 10 °C/min and a temperature scanning range from 40 °C to 1200 °C to measure samples for thermal stability, differential thermal curve and loss of sample weight during the heating up stage.

Results and discussion

The XRD analysis of kaolinite clay and the kaolinite clay catalyst :

The XRD analysis results of the sodium saturated kaolinite clay, but with non-calcination, are shown in Fig. 1(a). The XRD analysis results of various kaolinite clay catalysts after calcination at 350 °C are shown in Figs. 1(b) to 1(d), respectively. According to the results, a minor amount of quartz (about 37.7° for 2θ) and mica (about 24.9° for 2θ) contained kaolinite as indicated. Before the ingredients of kaolinite are transformed, by Bragg's law, $2d \sin\theta = n\lambda$, the research result reveal that the interfloor distance of the sodium saturated kaolinite with normal room temperature is 0.7177 nm. As it is modified by the positive ions and calcined to 350 °C, the interfloor distance of the kaolinite-Ag catalyst may shrink to 0.7167 nm, 0.7155 nm for kaolinite-Zn catalyst, and 0.7162 nm for kaolinite-Ti catalyst, respectively.

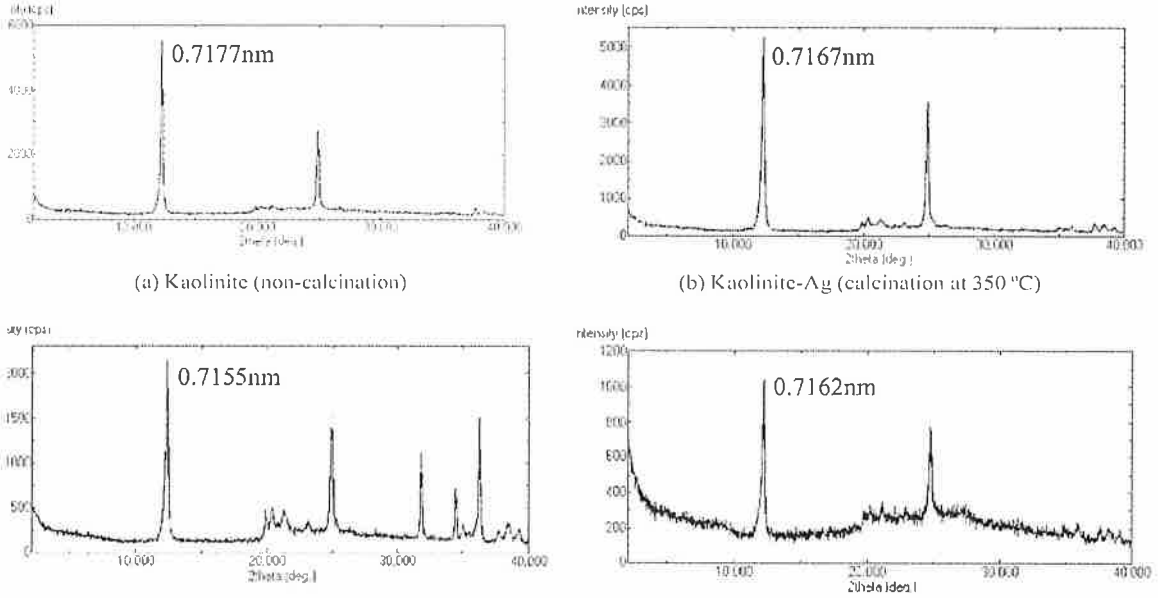

(a) Kaolinite (non-calcination)

(b) Kaolinite-Ag (calcination at 350 °C)

(c) Kaolinite-Zn (calcination at 350 °C)

(d) Kaolinite-Ti (calcination at 350 °C)

Fig. 1. The XRD analysis chart of kaolinite and kaolinite catalyst.

Kaolinite is a 1 to 1 type clay mineral with relatively weak plasticity, viscosity, contraction and expansion scales, as well as a non-expanding lattice. The junctions between kaolinite sheets (Lamella crystal flakes) are generally incomplete and contain monomolecular aquifers. As through the modification of various ions and sintering, water molecules will be dehydrated by heating, thus reducing the interfloor distance. Given the relative weak expansion scale of kaolinite, compared with other clay minerals in terms of expansion scales, it is obviously small[16].

TEM analysis of kaolinite clay and kaolinite catalyst :

This test aims to compare and examine the structures and statuses of kaolinite clay and kaolinite catalysts. Fig. 2 indicates the structure statuses of kaolinite clay and various catalysts. In Fig. 2(a), it is indicated that the crystallization particles of kaolinite are formed by mineral crystals in micro-flake shape that appear as hexagonal flat body (hexagonal crystal) with the diameters between 200 to 500 nm. It is hard to break into smaller and thinner crystal, hence, presenting close to perfect crystallinity[17]. The modified kaolinite-Ag catalyst is indicated in Fig. 2(b). From this display, it can be known that the distance between any single ions of the silver catalyst is between 30 to 80 nm. The appearance of silver ions shows a dark black color. It is quite possible that it contains a small portion of the metal oxide, i.e. silver oxide molecules, but most of them are still particles of silver ions with globe shape and tightly scattered.

The modified kaolinite-Zn catalyst is shown in Fig. 2(c). The zinc catalyst through high temperature sintering may contain a small portion of metal oxides like zinc oxide, but mainly it is still zinc ion particles with the diameter of about 30 to 100 nm. The modified kaolinite-Ti catalyst is shown in Fig. 2(d). The titanium catalysts

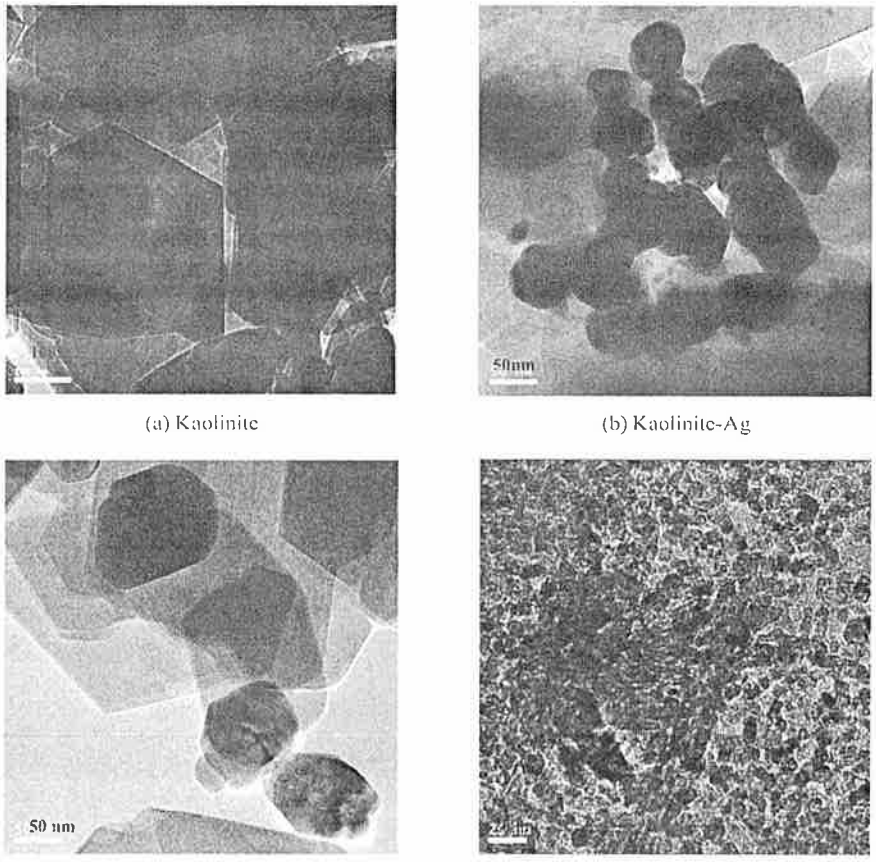

(a) Kaolinite (b) Kaolinite-Ag

(c) Kaolinite-Zn (d) Kaolinite-Ti

(a is the kaolinite structure after purification)

Fig. 2. The TEM analysis chart of kaolinite and kaolinite catalyst

are tightly scattered with obvious crystallization phenomena. It is expected that this titanium catalyst may also contain a small portion of TiO_2 particles, but the majority is still titanium ion particles. The size of individual titanium ion is approximately between 10 to 20 nm and also tightly scattered. It is proven by the results of the TEM analysis, noted above, that the distances between various catalyst particles and individual ions for different synthesized kaolinite catalysts are indeed nano-grade.

The dispersion display of elements contained by various kaolinite catalysts classified by the energy dispersive spectrometer (EDS) is shown in Fig. 3. The figure indicates that there are various positive ions after modification and certain ratios appeared through the various ion ingredients of the kaolinite catalyst.

The thermal analysis of kaolinite clay and kaolinite catalysts :

Fig. 4 indicates the results of the thermal analysis and thermogravimetric analysis by adopting nitrogen as the purging gas around the kaolinite clay with a heating up rate of 10 °C/min from 40 °C to 1200 °C. The differential thermal scanning calorimeter curve revealed that there are three endothermic peaks (melting peak) for kaolinite, which may separately appear at 77 °C, 530 °C and 1051 °C. And two exothermic peaks may also independently appear at 583 °C and 1009 °C. Given the multiple melting peaks indicated above, it reveals that kaolinite itself may have various crystal structures and microscopic phase patterns. In addition, this also indicates that certain relatively unstable crystals or crystal chips contained in kaolinite may first be melted at lower temperature, and then subsequently crystallized into more perfect crystals during the melting process[18]. As the temperature further increases, these crystals will be melted again, thus presenting a multiple melting peak phenomenon.

From the results of the thermogravimetric analysis, it is possible to know that kaolinite may have 11.8% weight loss between temperatures of 425 °C and 583 °C, and relatively less weight variations appear when the temperature is below 425 °C and above 583 °C. The endothermic peak at 530 °C accompanied with weight loss is due to the dehydration of the hydrate contained in the kaolinite. A relatively high ratio of weight loss may occur around this specific temperature. Subsequently, a phase

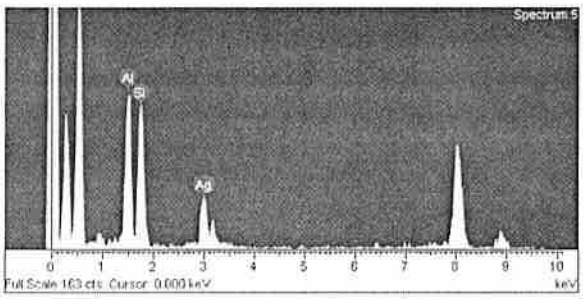

(a) Kaolinite-Ag

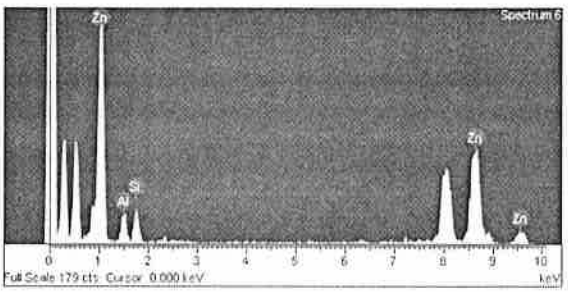

(b) Kaolinite-Zn

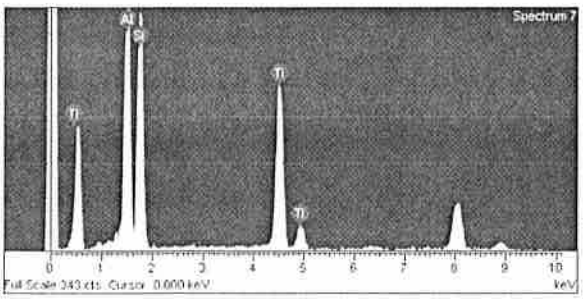

(c) Kaolinite-Ti

Fig. 3. The EDS analysis result of kaolinite catalyst.

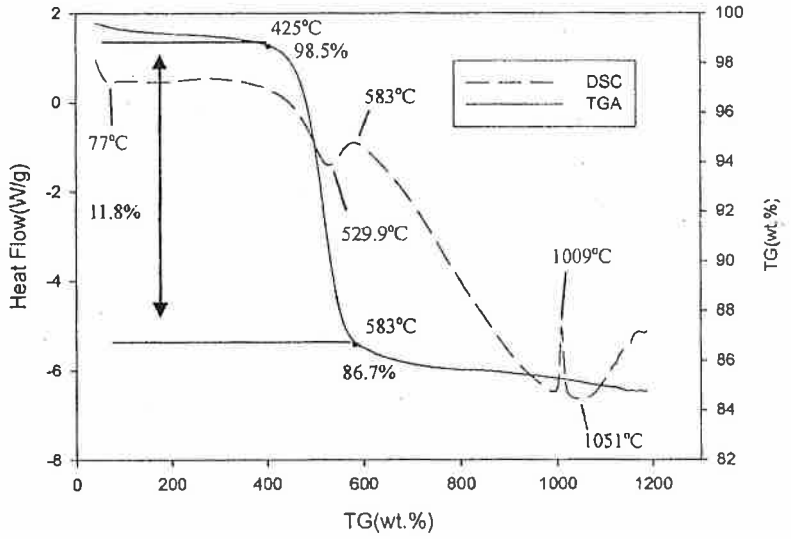

Fig. 4. DSC and TGA analysis chart of kaolinite clay.

shift may also occur to cause the kaolinite to become metakaolinite. The exothermic peak at 1009 °C occurs when the phase shifts by converting metakaolinite into primary mullite and the glass phase. The temperature for forming primary mullite in this study is slightly higher than the 980 °C noted by Chakraborty and Ghosh[19]. It is caused by the animosities of crystallinity and impurities contained by kaolinite so that it subsequently affects the temperature by forming primary mullite.

As for the kaolinite-Ag catalyst, endothermic peaks occur separately at 77 °C, 522 °C and 1051 °C. Exothermic peaks occur at 673 °C and 1009 °C, and the 11.9% weight loss takes place between 425 °C and 583 °C. The endothermic peak at 522 °C is very close to the temperature that appeared in the case of kaolinite; the accompanied weight loss is due to the dehydration process of the hydrate originally contained in the kaolinite. Subsequently, the kaolinite becomes metakaolinite after the phase transition. The exothermic peak at 673 °C has a delay of 90 °C compared with the temperature of kaolinite; the phase will change from metakaolinite into primary mullite (temperature is 1009 °C at this moment). It is speculated that the existence of silver ions between various layers of kaolinite cause the differences in crystallinity and the elements separately contained in kaolinite-Ag catalyst and the kaolinite itself. It leads to the formation temperature of mullite that can be slightly higher than kaolinite and the weight loss of kaolinite may gradually become stabilized.

As for the kaolinite-Zn catalyst, endothermic peaks occur separately at 77 °C, 562 °C, 837 °C and 1005 °C. Exothermic peaks occur at 628 °C and 969 °C correspondingly and the 10.7% weight loss takes place between 425 °C and 583 °C. It possible to determine from the figure that the endothermic peak accompanied weight loss occurred at 562 °C, and was caused by the dehydration process of hydrate originally contained by the kaolinite. Subsequently, the kaolinite becomes metakaolinite after phase transition. The exothermic peak at 628 °C has a delay of 5 °C as compared with the temperature of kaolinite, and the phase will be transferred from metakaolinite into primary mullite (temperature is 969 °C at this moment) and the weight loss may gradually be stabilized[20].

The endothermic peak at 837 °C is affected by the zinc ions, thus causing another melting point after this temperature. This result is almost the same as the temperature of the previous analysis result[1]. And the next endothermic peak (1005 °C) occurs at a lower temperature than kaolinite and kaolinite-Ag. The exothermic peak before 969 °C is possibly formed by the surface effect of kaolinite-Zn since the zinc ions on the kaolinite clay are pretty dense, thus before the kaolinite-Zn melted by the heating up process of the kaolinite-Zn structure, and may occur during the crystallization phenomenon and release heat. An exothermic peak will be formed and it is the phase transition for primary mullite as mentioned above[20].

As for the kaolinite-Ti catalyst, endothermic peaks occur separately at 77 °C, 518 °C, 890 °C and 1018 °C. Exothermic peaks occur at 595 °C and 1000 °C, respectively, and the 10% weight loss takes place between 405 °C and 583 °C. It possible to determine from the figure that the endothermic peak accompanied weight loss, which occurs at 518 °C, is caused by the dehydration process of hydrate originally contained in the kaolinite. Subsequently, the kaolinite becomes metakaolinite after the phase transition. The exothermic peak at 595 °C has a delay of 12 °C as compared with the temperature of kaolinite and the phase will be transferred from metakaolinite into primary mullite (the temperature is 1000 °C at this moment) and the weight loss may gradually stabilize as the phase transition towards primary mullite has started.

The endothermic peak at 837 °C is affected by the titanium ions, thus causing another endothermic peak to appear after this temperature. And the next endothermic peak (1018 °C) occurs at a lower temperature than kaolinite (1018 °C for kaolinite). The exothermic peak before this temperature at 1000 °C is possibly formed by the surface effect of kaolinite-Ti, since the titanium ions on the kaolinite clay have the same density as the zinc ions. Hence, before the kaolinite-Ti melted during the heating process, in the kaolinite-Ti structure a crystallization phenomenon may occur and release heat.

Conclusions

The modified clay catalysts verify the results of the TEM analysis in this study, that a range of catalyst particles of various synthesized kaolinite catalysts does fit nano-grade standards for the distances of their individual ions. Furthermore, after being classified by the EDS, the element dispersion situation of different kaolinite catalysts, certain ratios are shown by various ion ingredients of the kaolinite catalysts. According to the results of X-ray analysis, minor amounts of quartz (about 37.7° for 2θ) and mica (about 24.9° for 2θ) were contained in the kaolinite as indicated. As it is modified by the positive ions and calcined at 350 °C, the interfloor distance of the kaolinite-Ag catalyst may shrink to 0.7167 nm, 0.7155 nm for kaolinite-Zn catalyst, and 0.7144 nm for kaolinite-Ti catalyst, respectively. Finally, thermal analysis also revealed that there are three endothermic peaks (melting peaks) for kaolinite which may separately appear at 77 °C, 530 °C and 1051 °C. And two exothermic peaks may also independently appear at 583 °C and 1009 °C. Given the multiple melting peaks indicated above, it reveals that kaolinite itself may have various crystal structures and microscopic phase patterns.

References

1. J. Chen, X. Wen, X. Shi and R. Pan, *Environ. Eng. Sci.*, 2012, **29**, 392.
2. Z. Ding, G. Q. Lu and P. F. Greenfield, *J. Colloid Interf. Sci.*, 2000, **232**, 1.
3. J. J. Bang, L. E. Murr and E. V. Esquivel, *Mater. Charac.*, 2004, **52**, 1.
4. H. R. Chen, J. L. Shi, W. H. Zhang, M. L. Ruan and D. S. Yan, *Chem. Mater.*, 2001, **13**, 1035.
5. H. Masanori, N. Chiaki, O. Keisuke and I. Michio, *J. Am. Ceram. Soc.*, 2002, **85**, 1333.
6. J. M. Herrmann, H. Tahiri, Y. Ait-Ichou, G. Lassaletta, A. R. González-Elipe and A. Fernández, *Appl. Catal. B : Environ.*, 1997, **139**, 219.
7. T. Tsumura, N. Kojitani, H. Umemura, M. Toyoda and M. Inagaki, *Appl. Surf. Sci.*, 2000, **196**, 429.
8. N. Sobana, M. Muruganandam and M. Swaminathan, *Catal. Commun.*, 2008, **9**, 262.
9. F. J. Zhang, M. L. Chen and W. C. Oh, *Bull. Korean Chem. Soc.*, 2009, **30**, 1798.
10. K. Byrappa, A. S. Dayananda, C. P. Sajan, B. Basavalingu, M. B. Shayan, K. Soga and M. Yoshimura, *J. Mater. Sci.*, 2008, **43**, 2348.
11. P. Evans and D. W. Sheel, *Coat. Tech.*, 2007, **201**, 9319.
12. J. Tyczkowski, R. Kapica and J. Lojewska, *Thin Solid Film*, 2007, **515**, 6590.
13. L. Huang, S. P. Lau, H. Y. Yang and S. F. Yu, *Nanotechnology*, 2006, **17**, 1564.
14. W. D. Zhang, *Nanotechnology*, 2006, **17**, 1036.
15. J. J. Lee, J. W. Suh, J. S. Hong, J. M. Lee, Y. S. Lee and J. M. Park, *Mater. Sci. Forum*, 2008, **569**, 37.
16. M. A. Sainz, F. J. Serrano, J. M. Amigo, J. Bastida and A. Caballero, *J. Eur. Ceram. Soc.*, 2000, **20**, 403.
17. Y. F. Chen, M. C. Wang and M. H. Hon, *J. Mater. Res.*, 2004, **19**, 806.
18. N. H. Warner and J. D. Farmer, *Enviro. Eng. Sci.*, 2010, **10**, 523.
19. A. K. Chakraborty and D. K. Ghosh, *J. Am. Ceram. Soc.*, 1978, **61**, 1708.
20. O. S. Ahmed and K. Dutta, *J. Mole. Cat. A : Chemical*, 2005, **229**, 227.